

THE OPTICAL POTENTIAL FOR 99 MeV ${}^6\text{Li}$ SCATTERING

P. Schwandt, W. Jacobs, W. Ploughe,* M. Kaitchuck, J. Meek, P.P. Singh, F.D. Becchetti,** and J. Jänecke.**

With the recent availability of increased ${}^6\text{Li}$ beam intensities (of order 10-30 pA) on target, the 99 MeV ${}^6\text{Li}$ elastic-scattering angular distributions for ${}^{12}\text{C}$, ${}^{28}\text{Si}$, ${}^{40}\text{Ca}$, ${}^{58}\text{Ni}$, ${}^{90}\text{Zr}$ and ${}^{208}\text{Pb}$ previously reported¹⁾ have in most cases been extended to c.m. scattering angles near 50-55° (where the absolute cross section is of order 10 $\mu\text{b}/\text{sr}$ for all targets heavier than ${}^{12}\text{C}$). At the same time, the previous measurements were partially repeated to remove uncertainties and inconsistencies traceable in part to the very low (subnanoamp) beam intensities in the early experiments. Reliable charge integration possible at the present beam intensities allowed proper absolute normalization of the cross sections for all targets, while comparison of left-of-beam vs. right-of-beam scattering at forward angles established the 0° reference for all angular distributions to $\pm 0.1^\circ$. Zero-angle drifts in the beam were monitored by a pair of fixed detectors located at $\pm 14^\circ$.

These angular distributions have been analyzed in terms of a 6-parameter, complex, local optical-model potential with Woods-Saxon formfactors. The discrete potential-strength ambiguities commonly encountered for moderately or strongly absorbed projectiles at lower energies are still unresolved by the present higher-energy data. Largely equivalent fits are obtainable for real central

well depth V_0 between about 100 and 250 MeV at roughly 50 MeV intervals. We chose to fit all data with $V_0 = 95$ MeV (corresponding to a half-maximum radius of $1.30 A_T^{1/3}$ fm). The quality of fit generally obtained is represented by the example ${}^6\text{Li} + {}^{58}\text{Ni}$ in Fig. 1; the potential parameters indicated in that figure are also typical of those for most other targets.

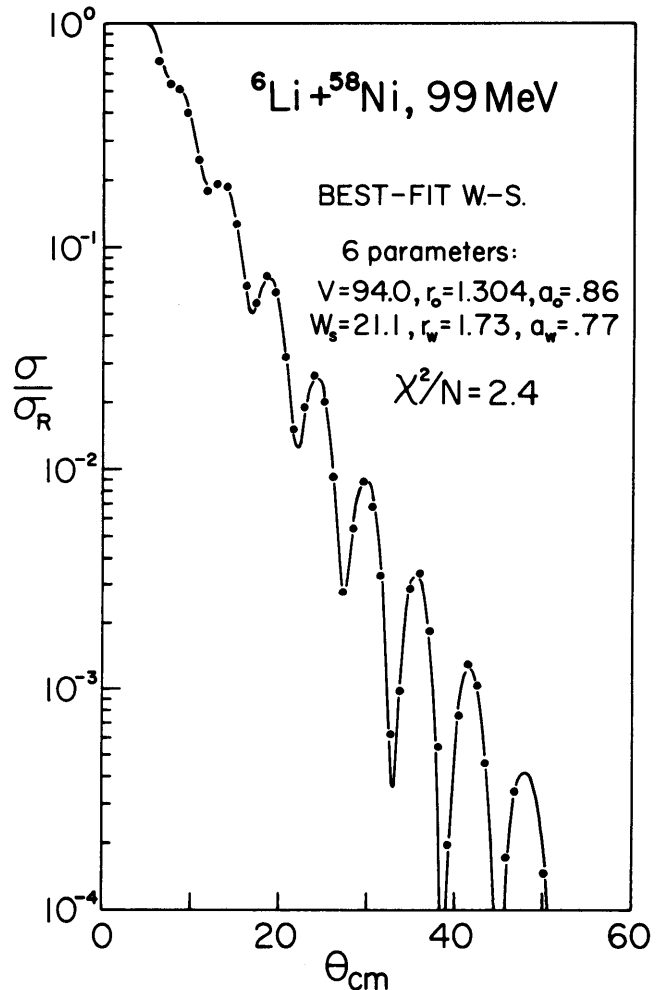


Figure 1

In view of the appreciable cluster probability of ${}^6\text{Li}$ as a weakly-bound $\alpha + d$ system, we have also attempted to describe the ${}^6\text{Li}$ elastic scattering within the framework of a simple cluster potential folding model. In terms of the well-known α -particle and deuteron optical potentials U_α , U_d we define the ${}^6\text{Li}$ optical potential as

$$U_{6\text{Li}}(R) = \int \{U_\alpha(|\vec{R}-\frac{1}{3}\vec{r}|) + U_d(|\vec{R}-\frac{2}{3}\vec{r}|)\} |X_{\alpha-d}(r)|^2 d\vec{r}$$

where $X_{\alpha-d}$ is the intercluster (α -d relative motion) function. Ignoring possible distortion of the cluster and its constituents in the nuclear field, we generated reasonable S-state model wavefunctions $X_{\alpha-d}$ from phenomenological $\alpha+d$ potentials which were required to reproduce correctly (1) the binding energy $E_B = 1.472$ MeV of ${}^6\text{Li}$ w.r.t. breakup into $\alpha+d$, (2) the empirical low-energy 3S_1 α -d scattering phase shifts,²⁾ and (3) the charge formfactor of the ${}^6\text{Li}$ ground state as determined from electron scattering.³⁾ Furthermore, in order to account phenomenologically for antisymmetrization effects at small α -d separation distances r , we required $X_{\alpha-d}$ to have the correct radial quantum number (e.g., a 2S state) and/or approach zero faster than r^2 as $r \rightarrow 0$ (e.g., by introducing a repulsive core in the potential). In Fig. 2, two such possible α -d bound state formfactors are illustrated: (a) represents a 2S state (with a node at 1.6 fm) in a real Woods-Saxon plus Coulomb potential $V_{\alpha-d}(r) = V_0 \{1 + \exp(\frac{r-R}{a})\}^{-1} + V_c(r)$ with $V_0 = -79.0$ MeV, $R = 1.83$ fm, $a = 0.70$ fm, and V_c due to a uniformly charged sphere of radius R ; (b) is a 1S Eckart

function $N(1-e^{-\alpha r})^3 \frac{1}{r} e^{-\kappa r}$, with $\alpha = .714$ and $\kappa^2 \equiv 2 \mu E_B / \hbar^2$, which is an eigenstate of the real potential with repulsive core $V_{\alpha-d}(r) = -44.4(e^{\alpha r}-1)^{-1} + 47.5(e^{\alpha r}-1)^{-2}$.

For U_α and U_d we chose phenomenological optical potentials⁴⁾ which fit elastic α and d scattering data at the appropriate energies $E_\alpha \approx \frac{2}{3} E_{\text{Li}}$, $E_d \approx \frac{1}{3} E_{\text{Li}}$. For ${}^{58}\text{Ni}$, the resulting folded ${}^6\text{Li}$ potential (real and imaginary central parts) is compared to the best-fit, 6-parameter Woods-Saxon potential in Fig. 3 (cf. Fig. 1 for the parameter values of the best-fit potential). The ${}^6\text{Li}$ folded potential is seen to be fairly insensitive to the particular choice of intercluster function $X_{\alpha-d}$. The generally good overall agreement of the imaginary potentials is very

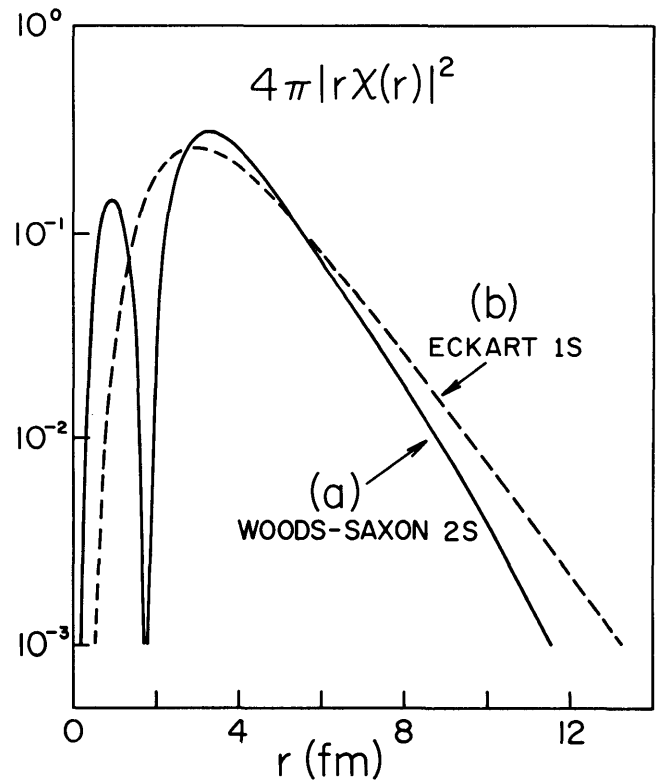


Figure 2

likely fortuitous since absorption modes clearly exist for ${}^6\text{Li}$ which cannot be accounted for by the superposition of α -particle and deuteron absorption. The real part of the folded ${}^6\text{Li}$ potential exhibits a somewhat rounder knee-region, but otherwise agrees remarkably well in shape with the phenomenological real potential. However, it is clearly too large in magnitude by about a factor of 2 everywhere, including the all-important surface region $4 < R < 7$ fm. This unexpectedly large and systematic overestimate of the real potential for ${}^6\text{Li}$ by the $\alpha+d$ cluster folding model has also

been found by Satchler and Love⁵⁾ for a double-folding model of the ${}^6\text{Li}$ potential in terms of a realistic effective 2-nucleon interaction which accounts reasonably well for heavier-ion scattering. A likely cause of the required renormalization in potential strength given by the two distinctly different folding-model approaches is the neglect of distortion and breakup of the ${}^6\text{Li}$ in the field of the target nucleus, although it is a priori not evident that such corrections should give a uniform scaling of the folded potentials or even have the correct sign (repulsive).

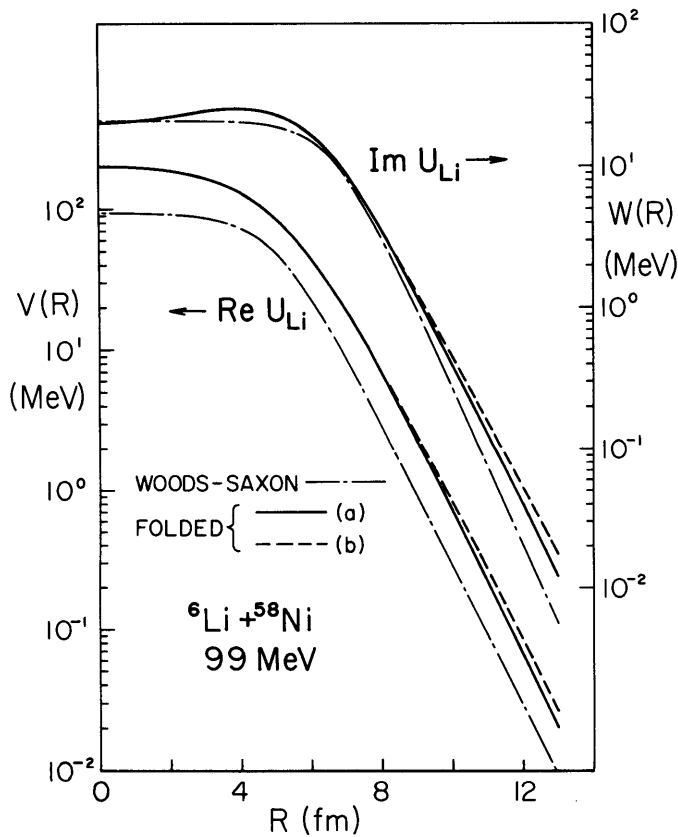


Figure 3

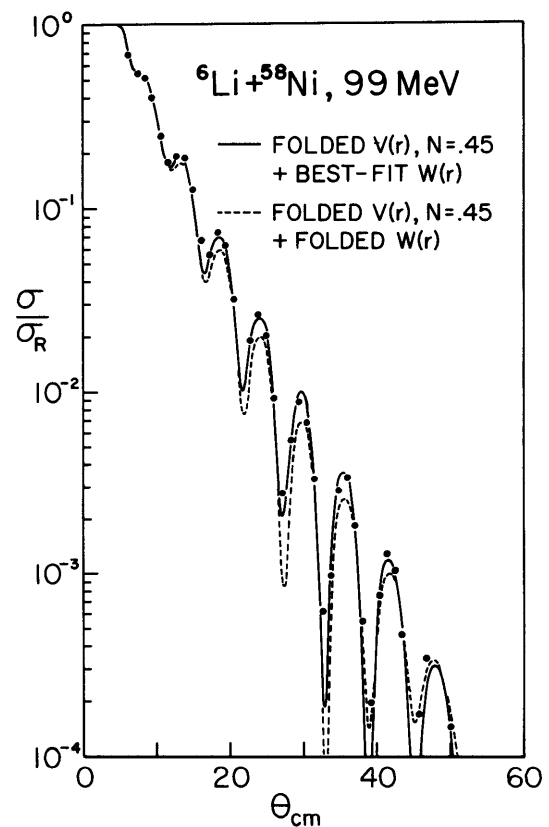


Figure 4

The 99 MeV ${}^6\text{Li} + {}^{58}\text{Ni}$ elastic scattering data were fitted with the real folded potential, which was allowed to be renormalized by a factor N , and using two forms of the imaginary potential: (1) the folded imaginary formfactor with strength adjusted for best 2-parameter fit, and (2) a Woods-Saxon imaginary potential with adjustable parameters (4-parameter fit). The results are illustrated in Fig. 4. A good fit is obtained in this case with $N = 0.45$ and a Woods-Saxon imaginary part (solid curve); the χ^2 -value is about twice that for the purely phenomenological 6-parameter Woods-Saxon fit of Fig. 1. The fit obtained with the folded imaginary potential (dashed curve) is considerably worse (χ^2 is 7 times larger than the best-fit value).

The conclusion we draw from this investigation is that although the cluster-folding model appears to produce the "correct" radial shape of the ${}^6\text{Li}$ real potential (in the sense that scattering data are well fit), the substantial, uniform renormalization of strength required indicates that the folding model in its present form (without breakup and other corrections) is too simplistic to provide a semi-microscopic basis for the phenomenological ${}^6\text{Li}$ potential.

*The Ohio State University, Columbus, Ohio 43210.

**University of Michigan, Ann Arbor, Michigan 48104.

1) P. Schwandt et al., IUCF Techn. and Scient. Report, Nov. 1975-Jan. 1977, p. 49 and BAPS 22, 633 (1977).

2) L.C. McIntyre and W. Haeberli, Nucl. Phys. 91, 382 (1967).

3) G.C. Li et al., Nucl. Phys. A162, 583 (1971).

4) J. Childs and W. Daehnick, BAPS 20 626 (1975); D.G. Madland et al., Phys. Rev. C9, 1002 (1974).

5) G.R. Satchler and W.G. Love, Physics Letters (in press).